EPSILON AURIGAE IN ECLIPSE: THE LIGHT AND COLOUR VARIATIONS

M. PARTHASARATHY and MARIAN L. FRUEH

Indian Institute of Astrophysics, Bangalore, India

and

McDonald Observatory and Department of Astronomy, University of Texas at Austin, Texas, U.S.A.

(Received 24 October, 1985)

Abstract. The *uvby* and *VRI* observations of ε Aur during the ingress and early totality phases obtained at the McDonald Observatory are analysed. The light and colour variations of ε Aur during the 1982–1984 eclipse are compared with those found during the 1955–1957 eclipse.

1. Introduction

Epsilon Aurigae is a long-period (P = 27.1 yr) eclipsing binary system consisting of a F0 Iae supergiant and an unseen slightly less massive companion. The primary eclipse is total with a depth of $0\overset{m}{.}80$. The duration of totality phase is 330 days. The secondary of ε Aur has been an enigma since the eclipse of 1928. The eclipse is peculiar because the spectrum during the totality is the same as that of the principal component (F0 Iae) and remains single throughout the orbital cycle. The eclipse depth is independent of wavelength whereas the depth and duration of the eclipse and masses of the components (Wright, 1970; Gyldenkerne, 1970; Kopal, 1971) implies that the components are almost equally bright and yet there is no secondary eclipse. The proposed models of the secondary range from a swarm of meteorites to a black hole (Ludendorff, 1924; Cameron, 1971). After the 1955 eclipse the earlier models (Kuiper *et al.*, 1937; Struve, 1956; Struve and Zebergs, 1962) of the secondary were replaced by three or four models. Kopal (1954, 1971) suggested that the secondary component of ε Aur is a disk-shaped object resembling the solar nebula. Kopal proposed that ε Aur constitutes a planetary system in the making and suggested that small variations in brightness during the totality phase are caused by protoplanetary-sized condensation in the disk. Huang (1965) proposed that the secondary is an opaque disk of cool material seen edge-on that completely obscures any hypothetical secondary star. Hack (1961) proposed that the secondary of ε Aur is a hot star resembling a late B-type dwarf surrounded by a shell or disk of ionized matter. In this model the wavelength independence of eclipse depth is explained as due to the electron scattering. Hack and Selvelli (1979) first observed UV excess. Plavec (1981) suggested that the UV excess may be associated with the accretion disk of the secondary. Cameron (1971) and Wilson (1971) suggested that the secondary of ε Aur is a black hole with an extensive accretion disk.

The spectroscopic and photometric results of the 1955 eclipse were discussed by Wright (1970), Gyldenkerne (1970), and Sahade and Wood (1978). The 1982–1984

Astrophysics and Space Science **123** (1986) 31–48.

eclipse of ε Aur was the first to be extensively studied in the wavelength regions from far ultraviolet to far infrared. Chapman *et al.* (1983), Parthasarathy and Lambert (1983c), and Boehm *et al.* (1984) have discussed the IUE spectra of ε Aur eclipse covering the periods of ingress and totality. Backman *et al.* (1984) discussed the results of IR photometry of ε Aur from 1 to 20 μ.

In this paper we present an analysis of our *uvby* and *VRI* observations of ε Aur made during the ingress and early totality phases of the 1982–1984 eclipse, and compare the light and colour variations with those found during the 1955–1957 eclipse.

2. Observations

uvby and *VRI* observations of ε Aur were obtained on 28 nights between April 1982 and April 1983, with the 76 cm reflector telescope of the McDonald Observatory. λ Aur was used as the primary comparison star. Observations were made through the standard set of *uvby* and *VRI* filters. Standard stars from the lists of Barnes and Moffett (1979) and Moffett and Barnes (1979) were observed. Most of the observations were obtained after late August 1982; the effects from the eruptions of El Chichon on the atmospheric extinction measurements continued to diminish gradually (see *Bull. Am. Astron. Soc.* **16**, 336, 1984). The monthly mean visual extinction k_v values from late August 1982 differed by $0\overset{m}{.}10$ to $0\overset{m}{.}05$ from the monthly mean k_v values listed by de Vaucouleurs and Angione (1974), for the period 1960–1968. After atmospheric extinction corrections the data are transformed to the standard system. The differential *uvby* and *VRI* magnitudes (ε Aur–λ Aur) are listed in Tables I and II.

3. Light Curves

The differential *uvby* and *VRI* observations (ε Aur–λ Aur) are plotted in Figures 1 and 2. Our observations cover the ingress and early totality phase of ε Aur. The *V* filter observations are in good agreement with the *V* filter data of ε Aur obtained at the Hopkins Phoenix Observatory, Arizona (HPO) and the Tjornisland Astronomical Observatory in Sweden (TAO) (Hopkins and Stencel, 1983). In Figure 3 we show the McDonald V data together with the HPO and TAO V data from Hopkins and Stencel (1983) and the data of Flin *et al.* (1985). The TAO and HPO data are selected because of their close match and good coverage of the eclipse phase. It is clear from Figure 3 that the McDonald V data matches very well with the TAO and HPO data. At the time of writing this paper we do not have the ε Aur Newletter Nos. 11, 12, ..., to include in Figure 3 the HPO and TAO data of the post mid-eclipse and egress phases. The data of Flin *et al.* (1985) is of unequal quality and appears to be not as good as TAO and HPO data.

3.1. Contact times of the eclipse

From an analysis of previous eclipse light curves Gyldenkerne (1970) predicted the dates of contacts for the 1982–1984 eclipse; ε Aur was in eclipse as expected from the times

TABLE I

uvby observations (ε Aurigae–λ Aurigae)

JD (Hel.) 2440000+	*u*	*v*	*b*	*y*
5207.9174	− 1.062	− 1.748	− 1.547	− 1.578
5207.9193	− 1.031	− 1.747	− 1.562	− 1.589
5208.8814	− 1.041	− 1.741	− 1.555	− 1.560
5208.8820	− 1.022	− 1.721	− 1.551	− 1.577
5211.8771	− 0.996	− 1.698	− 1.529	− 1.557
5211.8800	− 1.010	− 1.683	− 1.522	− 1.539
5211.8817	− 0.993	− 1.700	− 1.521	− 1.546
5211.8833	− 0.995	− 1.708	− 1.526	− 1.563
5217.8956	− 0.887	− 1.617	− 1.440	− 1.478
5217.8978	− 0.898	− 1.602	− 1.445	− 1.471
5217.8996	− 0.904	− 1.634	− 1.452	− 1.485
5218.8977	− 0.861	− 1.595	− 1.421	− 1.458
5218.8992	− 0.870	− 1.590	− 1.434	− 1.475
5218.9008	− 0.860	− 1.601	− 1.421	− 1.457
5219.8944	− 0.862	− 1.602	− 1.416	− 1.448
5219.8969	− 0.860	− 1.585	− 1.415	− 1.459
5219.8987	− 0.849	− 1.587	− 1.422	− 1.455
5226.8563	− 0.803	− 1.507	− 1.341	− 1.366
5226.8580	− 0.808	− 1.503	− 1.343	− 1.384
5226.8615		− 1.509	− 1.345	− 1.379
5227.8576	− 0.769	− 1.486	− 1.309	− 1.376
5227.8592	− 0.773	− 1.485	− 1.330	− 1.367
5227.8609	− 0.759	− 1.488	− 1.330	− 1.365
5227.8626	− 0.753	− 1.485	− 1.322	− 1.362
5229.8684	− 0.775	− 1.487	− 1.316	− 1.357
5229.8702	− 0.758	− 1.473	− 1.317	− 1.347
5229.8722	− 0.745	− 1.482	− 1.312	− 1.351
5230.8786	− 0.718	− 1.450	− 1.289	− 1.321
5230.8803	− 0.718	− 1.452	− 1.289	− 1.330
5230.8819	− 0.713	− 1.442	− 1.299	− 1.329
5255.9797	− 0.535	− 1.335	− 1.171	− 1.207
5255.9821	− 0.531	− 1.338	− 1.169	− 1.201
5255.9836	− 0.538	− 1.333	− 1.171	− 1.199
5255.9852	− 0.531	− 1.336	− 1.173	− 1.203
5256.7812	− 0.610	− 1.344	− 1.185	− 1.203
5256.7853	− 0.607	− 1.341	− 1.177	− 1.203
5256.7874	− 0.596	− 1.344	− 1.180	− 1.211
5256.7891	− 0.587	− 1.321	− 1.175	− 1.205
5257.8271	− 0.576	− 1.330	− 1.156	− 1.203
5257.8292	− 0.574	− 1.341	− 1.170	− 1.200
5257.8321	− 0.570	− 1.335	− 1.175	− 1.205
5257.8326	− 0.567	− 1.338	− 1.169	− 1.209

Table I (continued)

JD (Hel.) 2440000+	*u*	*v*	*b*	*y*
5258.8067	−0.542	−1.321	−1.164	−1.204
5258.8117	−0.554	−1.330	−1.158	−1.205
5278.7107	−0.554	−1.235	−1.081	−1.111
5278.7125	−0.539	−1.232	−1.072	−1.105
5278.7142	−0.549	−1.238	−1.073	−1.110
5278.7159	−0.535	−1.234	−1.078	−1.107
5279.8839	−0.462	−1.231	−1.059	−1.099
5279.8858	−0.468	−1.227	−1.062	−1.094
5279.875	−0.461	−1.221	−1.061	−1.099
5282.8657	−0.444	−1.205	−1.048	−1.079
5282.8671	−0.441	−1.207	−1.037	−1.083
5282.8685	−0.443	−1.204	−1.042	−1.086
5282.8698	−0.439	−1.202	−1.041	−1.086
5343.5895	−0.331	−1.119	−0.948	−0.990
5343.5912	−0.326	−1.115	−0.948	−0.992
5343.5933	−0.328	−1.113	−0.945	−0.988
5343.5950	−0.332	−1.116	−0.953	−0.991
5343.7240	−0.293	−1.108	−0.952	−0.992
5343.7255	−0.296	−1.120	−0.945	−0.988
5343.7270	−0.294	−1.122	−0.949	−0.989
5343.7286	−0.294	−1.120	−0.948	−0.987
5343.8321	−0.284	−1.115	−0.946	−0.987
5343.8336	−0.276	−1.108	−0.948	−0.978
5343.8350	−0.285	−1.114	−0.949	−0.995
5343.8365	−0.289	−1.110	−0.949	−0.979
5344.6119	−0.316	−1.111	−0.945	−0.983
5344.6141	−0.318	−1.131	−0.947	−0.985
5344.6160	−0.308	−1.114	−0.948	−0.990
5344.6176	−0.319	−1.113	−0.951	−0.994
5383.5841	−0.310	−1.078	−0.917	−0.950
5383.5863	−0.315	−1.075	−0.908	−0.949
5383.5879	−0.313	−1.075	−0.906	−0.951
5383.5899	−0.311	−1.076	−0.915	−0.951
5383.5916	−0.317	−1.082	−0.913	−0.952
5394.6395	−0.245	−1.054	−0.892	−0.921
5394.6418	−0.249	−1.055	−0.881	−0.926
5394.6472	−0.236	−1.051	−0.887	−0.924
5394.6489	−0.233	−1.058	−0.884	−0.918
5394.6516	−0.241	−1.053	−0.890	−0.928
5394.6544	−0.238	−1.053	−0.886	−0.926
5400.6044	−0.249	−1.055	−0.895	−0.920
5400.6060	−0.241	−1.047	−0.885	−0.928
5400.6077	−0.246	−1.060	−0.884	−0.930
5400.6101	−0.233	−1.057	−0.876	−0.920

Table I (continued)

JD (Hel.) 2440000+	*u*	*v*	*b*	*y*
5402.6062	−0.259	−1.065	−0.892	−0.926
5402.6098	−0.265	−1.061	−0.894	−0.929
5402.6114	−0.262	−1.063	−0.871	−0.889
5402.6130	−0.246	−1.053	−0.884	−0.882
5417.6451	−0.196	−1.060	−0.896	−0.931
5417.6467	−0.198	−1.059	−0.885	−0.942
5417.6482	−0.207	−1.056	−0.884	−0.946
5417.6514	−0.197	−1.049	−0.888	−0.919
5425.6063	−0.213	−1.077	−0.921	−0.956
5425.6090	−0.207	−1.082	−0.919	−0.967
5425.6098	−0.205	−1.074	−0.916	−0.953
5425.6093	−0.228	−1.062	−0.907	−0.954

of contact given by Gyldenkerne. However, the predicted times of contact and observed times of contact are found to differ slightly.

There are not enough pre-eclipse (just before the first contact) photometric data available to determine the date of first contact accurately, and the Cepheid-like pulsation of the primary also introduces uncertainty in the determination of times of contact. From the eclipse light curves of Figures 1, 2, and 3 and from the pre-eclipse photometry published in the ε Aur Newsletter 9, we estimated the date of first contact to be JD 2445170. The V magnitude around this time is $V = 3.11$. The mean V magnitude of ε Aur outside eclipse given in the literature is $V = 3.0$. The light variations near the second contact are well observed and there are enough data to determine the time of contact reasonably well. The date of second contact is determined to be JD 2445300. The second contact took place 15 days earlier than predicted. If we assume that the duration of ingress phase of the eclipse remained the same as that found during the 1955 eclipse (135 days; see Gyldenkerne, 1970) then the date of first contact is JD 2445165.

The duration of ingress could vary from eclipse to eclipse. Gyldenkerne (1970) and Larsson-Leander (1958) derived 182 days for the duration of the ingress phase based on the eclipses before the 1955 eclipse. We estimated the duration of the ingress phase during the 1982–1984 eclipse to be 129 days, which is slightly smaller than that found for the 1955 eclipse. However, in view of the long orbital period and uncertainties concerning the mean brightness values for the pre-eclipse and totality we may conclude that the duration of the ingress phase has not changed significantly and is the same as that found for the 1955 eclipse. We used the Oki *et al.* (1984), Boyd *et al.* (1984), and Flin *et al.* (1985) light curves to estimate the time of third contact.

Oki *et al.* and Boyd *et al.* reported brightening near third contact. The brightening continued for 40 days (JD 2445700–2445740). The maximum brightening occurred on

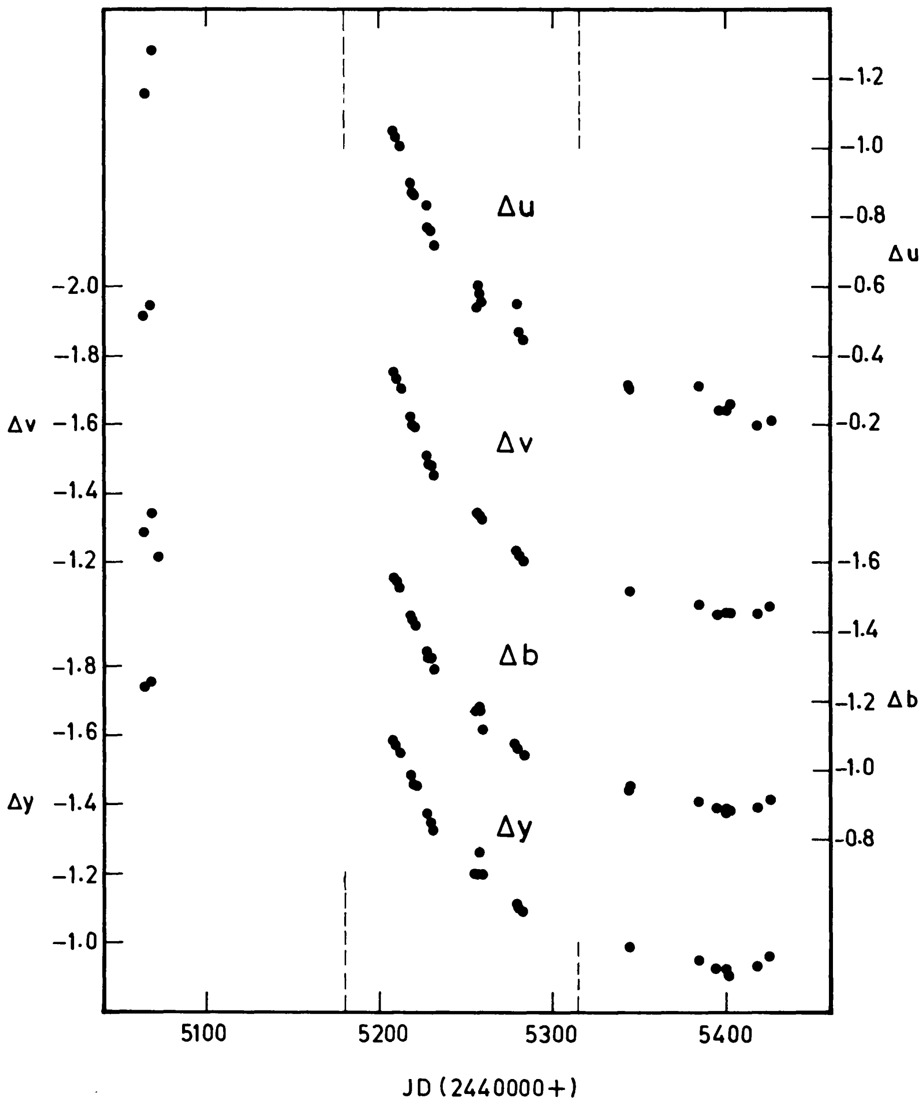

Fig. 1. The *uvby* light curves of ε Aur during the ingress and early totality phases according to observations at the McDonald Observatory. The dashed vertical lines indicate the predicted times of first and second contacts.

JD 2445709 which coincides with the predicted time of the third contact. We estimated the times of the third contact to be JD 2445735, JD 2445740, JD 2445748 in *V*, *B*, and *U*, respectively.

The amplitude of brightening in *U* near the third contact is large, $0\overset{m}{.}2$, and there was a delay of almost 25 days before the recovery began. The amplitude in *V* is $0\overset{m}{.}04$. We adopt the time of third contact to be JD 2445740. The brightening near the third contact appears to have introduced uncertainty in the exact date of third contact. We find the duration of totality phase in the 1982–1984 eclipse of ε Aur to be 440 days, which is slightly longer than that found during the previous eclipses. Gyldenkerne (1970) gives duration of totality phase in the 1955–1957 eclipse and the mean of previous eclipses

TABLE II

VRI observations (ε Aurigae–λ Aurigae)

JD (Hel.) 2440000 +	*V*	*R*	*I*
5207.9288	– 1.566	– 1.576	– 1.539
5207.9306	– 1.547	– 1.567	– 1.529
5207.9321	– 1.590	– 1.575	– 1.554
5207.9338	– 1.581	– 1.561	– 1.545
5208.8710	– 1.605	– 1.615	– 1.578
5208.8728	– 1.599	– 1.593	– 1.571
5208.8744	– 1.597	– 1.623	– 1.555
5208.8759	– 1.617	– 1.615	– 1.588
5208.8727	– 1.615	– 1.599	– 1.570
5209.9077	– 1.594	– 1.591	– 1.543
5209.9095	– 1.603	– 1.591	– 1.564
5209.9110	– 1.609	– 1.601	– 1.571
5209.9114	– 1.607	– 1.595	– 1.546
5209.9139	– 1.570	– 1.573	– 1.550
5209.9154	– 1.589	– 1.592	– 1.549
5209.9174	– 1.584	– 1.585	– 1.545
5209.9192	– 1.590	– 1.578	– 1.533
5209.9207	– 1.593	– 1.606	– 1.550
5209.9225	– 1.592	– 1.600	– 1.559
5209.9240	– 1.611	– 1.603	– 1.568
5209.9278	– 1.586	– 1.589	– 1.547
5209.9295	– 1.586	– 1.561	– 1.544
5209.9309	– 1.587	– 1.590	– 1.555
5209.9324	– 1.576	– 1.588	– 1.543
5209.9339	– 1.581	– 1.575	– 1.536
5209.9354	– 1.593	– 1.592	– 1.536
5209.9369	– 1.605	– 1.567	– 1.540
5209.9386	– 1.591	– 1.589	– 1.539
5209.9400	– 1.589	– 1.597	– 1.549
5209.9415	– 1.587	– 1.589	– 1.552
5209.9429	– 1.592	– 1.602	– 1.549
5209.9444	– 1.578	– 1.593	– 1.543
5211.8771	– 1.582	– 1.576	– 1.559
5211.8712	– 1.587	– 1.591	– 1.548
5211.8728	– 1.592	– 1.573	– 1.540
5211.8745	– 1.583	– 1.593	– 1.554
5217.8865	– 1.495	– 1.504	– 1.471
5217.8881	– 1.503	– 1.491	– 1.472
5217.8902	– 1.500	– 1.501	– 1.477
5217.8919	– 1.503	– 1.504	– 1.475
5218.8558	– 1.481	– 1.472	– 1.466
5218.8584	– 1.499	– 1.474	– 1.470
5218.8929	– 1.498	– 1.483	– 1.458
5218.8944	– 1.473	– 1.492	– 1.459
5219.8888	– 1.469	– 1.482	– 1.455
5219.8904	– 1.471	– 1.472	– 1.439
5219.8917	– 1.466	– 1.478	– 1.447
5226.8469	– 1.386	– 1.402	– 1.378
5226.8493	– 1.408	– 1.406	– 1.384
5226.8510	– 1.397	– 1.395	– 1.376
5226.8525	– 1.394	– 1.391	– 1.366
5227.8397	– 1.383	– 1.395	– 1.385
5227.8418	– 1.381	– 1.382	– 1.357
5227.8433	– 1.384	– 1.380	– 1.349
5227.8448	– 1.387	– 1.392	– 1.366
5229.8568	– 1.367	– 1.380	– 1.343
5229.8585	– 1.365	– 1.374	– 1.342
5229.8600	– 1.366	– 1.367	– 1.350
5229.8677	– 1.367	– 1.374	– 1.342
5230.8660	– 1.356	– 1.361	– 1.335
5230.8677	– 1.355	– 1.362	– 1.331
5230.8695	– 1.353	– 1.360	– 1.330
5230.8715	– 1.352	– 1.367	– 1.339
5232.8575	– 1.349	– 1.341	– 1.317
5232.8593	– 1.363	– 1.354	– 1.365
5232.8608	– 1.361	– 1.367	– 1.346
5255.9727	– 1.217	– 1.216	– 1.196
5255.9743	– 1.221	– 1.212	– 1.193
5255.9757	– 1.218	– 1.214	– 1.188
5255.9771	– 1.222	– 1.207	– 1.193
5257.8064	– 1.222	– 1.218	– 1.205
5257.8091	– 1.224	– 1.222	– 1.190
5257.8107	– 1.222	– 1.224	– 1.187
5257.8122	– 1.223	– 1.219	– 1.194
5257.8136	– 1.231	– 1.222	– 1.201
5258.7863	– 1.224	– 1.221	– 1.206
5258.7877	– 1.215	– 1.229	– 1.211
5258.7895	– 1.219	– 1.223	– 1.205
5258.7908	– 1.219	– 1.219	– 1.197
5260.7747	– 1.215	– 1.218	– 1.199
5260.7764	– 1.220	– 1.223	– 1.200
5260.7782	– 1.218	– 1.222	– 1.195
5260.7796	– 1.217	– 1.218	– 1.201
5278.6990	– 1.131	– 1.129	– 1.116
5278.7018	– 1.118	– 1.116	– 1.104
5278.7043	– 1.128	– 1.125	– 1.109
5278.7065	– 1.122	– 1.129	– 1.104

Table II (continued)

JD (Hel.) 2440000+	V	R	I
5279.8719	−1.109	−1.109	−1.093
5279.8759	−1.116	−1.108	−1.084
5279.8776	−1.104	−1.104	−1.088
5279.8797	−1.114	−1.112	−1.088
5282.8535	−1.093	−1.094	−1.079
5282.8561	−1.094	−1.090	−1.069
5282.8581	−1.089	−1.087	−1.066
5282.8598	−1.087	−1.091	−1.073
5342.6501	−1.002	−1.001	−0.981
5342.6523	−0.995	−1.007	−0.985
5342.6538	−1.004	−0.991	−0.986
5342.6555	−1.000	−1.001	−0.987
5342.6570	−0.996	−1.002	−0.984
5342.6585	−0.993	−0.999	−0.981
5342.6600	−0.992	−0.999	−0.990
5342.6618	−0.993	−0.991	−0.981
5342.6634	−0.996	−0.997	−0.987
5342.6650	−0.996	−0.999	−0.982
5342.6666	−0.990	−0.998	−0.989
5342.6686	−0.999	−0.997	−0.974
5342.6758	−1.000	−0.993	−0.980
5342.6773	−0.993	−0.996	−0.971
5342.6791	−0.996	−0.998	−0.983
5342.6810	−0.992	−0.993	−0.982
5342.6825	−0.999	−0.994	−0.983
5342.6840	−0.996	−0.999	−0.991
5342.6861	−0.998	−0.996	−0.988
5342.6877	−0.998	−0.995	−0.977
5342.6891	−1.000	−0.999	−0.982
5342.6906	−0.997	−0.998	−0.988
5342.6921	−1.003	−0.988	−0.974
5342.6935	−0.996	−1.003	−0.981
5342.6950	−0.996	−0.997	−0.981
5343.5982	−0.998	−1.001	−0.982
5343.6004	−1.001	−1.001	−0.987
5343.6024	−1.001	−0.995	−0.983
5343.6042	−0.997	−1.001	−0.986
5343.6057	−1.003	−1.001	−0.986
5343.6075	−0.997	−1.001	−0.987
5343.6090	−0.994	−0.998	−0.989
5343.6106	−0.999	−0.999	−0.987
5343.6120	−0.997	−1.000	−0.991
5343.6134	−1.002	−1.000	−0.984
5343.6149	−0.996	−0.998	−0.980
5343.6165	−0.996	−1.001	−0.981
5343.6181	−1.003	−1.000	−0.986
5343.6199	−0.996	−1.002	−0.985
5343.6215	−0.997	−0.999	−0.981
5343.6230	−1.001	−1.000	−0.986
5343.6244	−0.996	−0.998	−0.983
5343.6358	−0.999	−0.999	−0.989
5343.6272	−0.996	−0.998	−0.983
5343.6285	−0.999	−1.000	−0.983
5343.7085	−0.997	−0.995	−0.979
5343.7103	−0.995	−0.996	−0.981
5343.7141	−0.997	−0.996	−0.980
5343.7154	−0.997	−0.995	−0.976
5343.7168	−0.995	−0.995	−0.976
5343.7181	−0.996	−0.997	−0.987
5343.7194	−0.997	−0.996	−0.983
5343.7207	−0.995	−0.996	−0.981
5343.8244	−1.001	−0.997	−0.971
5343.8258	−0.991	−0.997	−0.976
5343.8273	−0.995	−0.996	−0.974
5343.8286	−0.993	−0.990	−0.975
5344.6211	−0.991	−0.991	−0.983
5344.6227	−1.001	−0.995	−0.975
5344.6241	−1.001	−0.992	−0.982
5344.6255	−0.991	−0.998	−0.984
5383.5949	−0.958	−0.960	−0.954
5383.5965	−0.959	−0.962	−0.947
5383.5981	−0.962	−0.960	−0.948
5383.6001	−0.954	−0.960	−0.948
5383.6017	−0.956	−0.955	−0.949
5383.6033	−0.961	−0.957	−0.938
5383.6047	−0.966	−0.958	−0.947
5383.6060	−0.963	−0.960	−0.943
5383.6075	−0.957	−0.964	−0.953
5383.6092	−0.962	−0.959	−0.951
5383.6109	−0.955	−0.962	−0.951
5383.6126	−0.961	−0.957	−0.945
5383.6144	−0.957	−0.960	−0.949
5383.6161	−0.961	−0.962	−0.948
5383.6190	−0.957	−0.964	−0.941
5383.6331	−0.957	−0.961	−0.954
5383.6352	−0.952	−0.954	−0.947
5383.6368	−0.957	−0.955	−0.953
5383.6383	−0.954	−0.961	−0.944
5383.6399	−0.961	−0.958	−0.941
5383.6414	−0.958	−0.956	−0.941
5394.6590	−0.936	−0.927	−0.920
5394.6623	−0.933	−0.933	−0.914
5394.6678	−0.931	−0.926	−0.914
5394.6694	−0.925	−0.932	−0.909

Table II (continued)

JD (Hel.) 2440000+	*V*	*R*	*I*	JD (Hel.) 2440000+	*V*	*R*	*I*
5400.5947	−0.934	−0.927	−0.903	5417.6126	−0.946	−0.952	−0.939
5400.5963	−0.927	−0.924	−0.926	5417.6141	−0.929	−0.939	−0.924
5400.5979	−0.933	−0.925	−0.911	5417.6155	−0.912	−0.931	−0.918
5400.5993	−0.938	−0.928	−0.914	5417.6171	−0.948	−0.934	−0.926
5400.6009	−0.939	−0.928	−0.917	5417.6188	−0.960	−0.933	−0.922
5402.6170	−0.933	−0.927	−0.908	5425.5977	−0.985	−0.977	−0.958
5402.6192	−0.936	−0.927	−0.916	5425.5993	−0.962	−0.960	−0.960
5402.6210	−0.934	−0.928	−0.912	5425.6010	−0.944	−0.954	−0.948
5402.6230	−0.935	−0.930	−0.913	5425.6024	−0.986	−0.981	−0.966
5402.6244	−0.935	−0.928	−0.911	5425.6038	−0.950	−0.972	−0.973

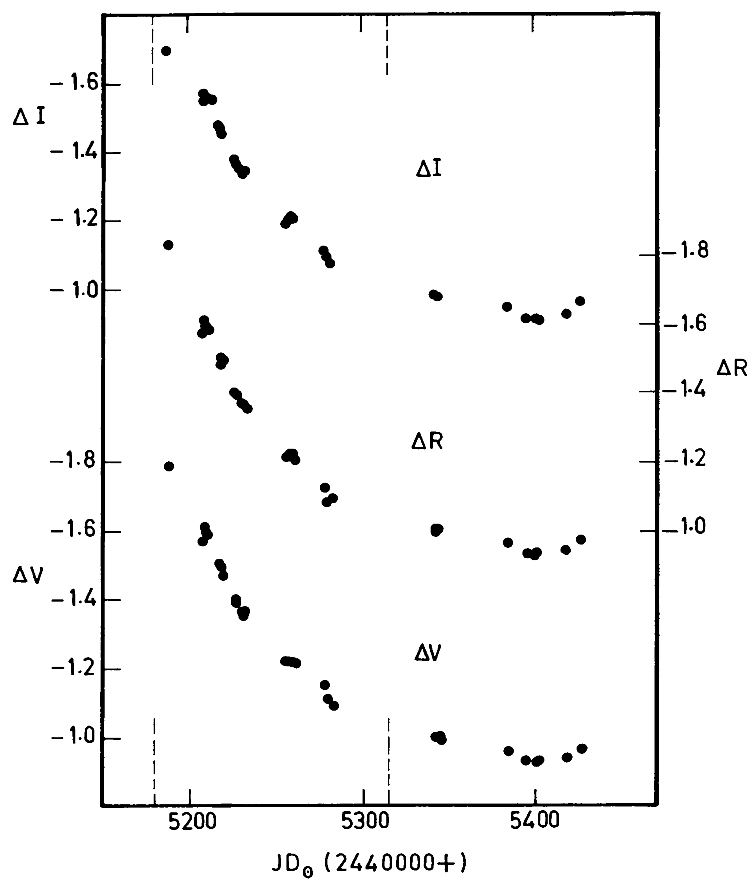

Fig. 2. The *VRI* light curves of ε Aur during the ingress and early totality phases according to observations at the McDonald Observatory. The dashed vertical lines indicate the predicted times of first and second contacts.

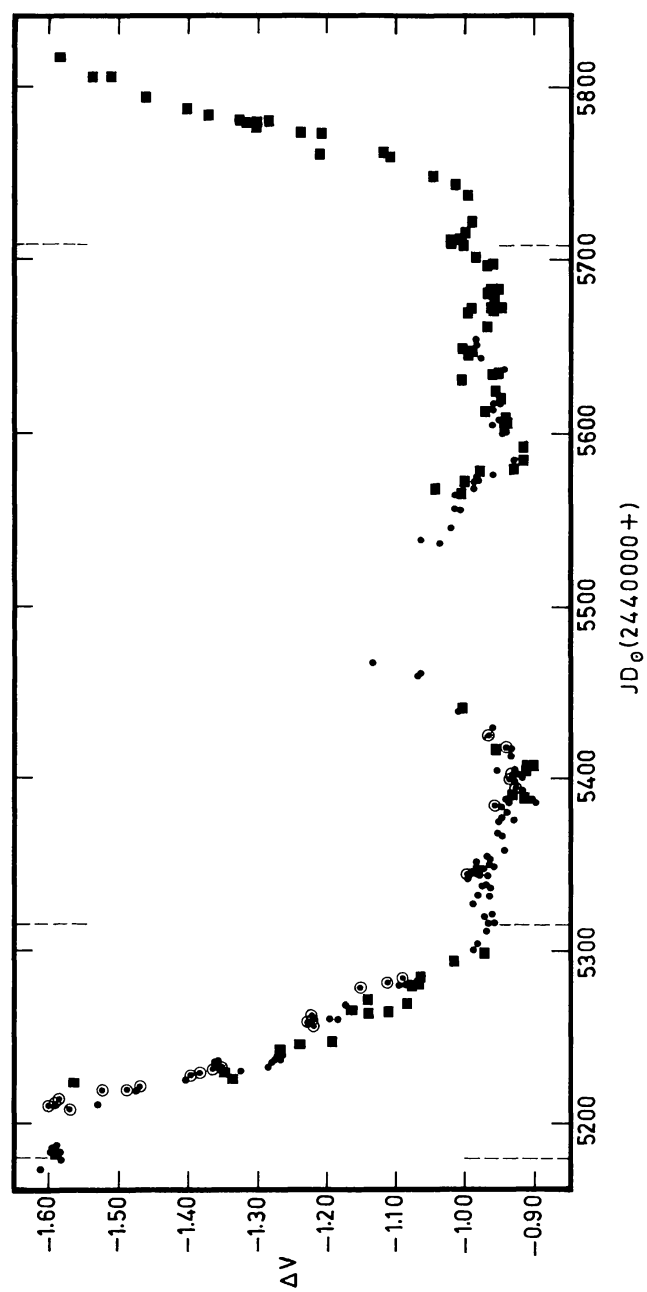

Fig. 3. The V light curve of ε Aur during ingress, totality and egress phases. ⊙: McDonald Observatory; ●: Hopkins Phoenix Observatory (HPO), and Tjornisland Astronomical Observatory (TAO); ■: Jagiellonian University Observatory. The dashed vertical lines indicate the predicted times of first, second, and third contacts.

TABLE III

Dates of contact of the 1982–1984 eclipse

	Predicted		Observed
	Date	JD	JD
1st Contact	29 July, 1982	2445180	2445165
2nd Contact	11 Dec.,1982	2445315	2445300
3rd Contact	9 Jan., 1982	2445708	2445740
4th Contact	29 May,1982	2445850	(2445890)

to be 394 days and 330 days, respectively. In Table III we list the observed and predicted dates of contact. The fourth contact and mid-eclipse took place when ε Aur is not accessible for observations. The uncertainty in the date of the fourth contact can be large. However, the duration of ingress and egress phases of the 1982–1984 eclipse are not very much different from the 1955–1957 eclipse. In Table IV we have listed the duration of various phases of the 1982–1984 eclipse and those of previous eclipses. The gradual lengthening of the duration of totality may be due to a slow expansion of the disk. The difference in the dates of second contact of the 1955–1957 eclipse and 1982–1984 eclipse give a period of 9870 days.

TABLE IV

The duration of eclipse phases

	Eclipse 1982–1984	Eclipse 1955–1957	Mean of eclipses prior to 1955
Duration of totality	440 days	394 days	330 days
Duration of ingress	135	135	182
Duration of egress	~150	141	203
Duration of eclipse	725	670	714

3.2. The Light Variations during the Totality

The light variations of ε Aur during the totality phase in the 1982–1984 eclipse (see Figure 3) are not exactly similar to those found in 1955–1957 and 1928 eclipses. The interesting aspects are: (i) the mid-eclipse brightening; (ii) the anomalous brightening near third contact; (iii) the long duration of the totality; and (iv) the downward slope of the light variations during the totality from second contact to third contact. The mid-eclipse brightening started around JD 2445410 and ended around JD 2445580. The duration of this phase is about 170 days. In Figure 4 we have superimposed the 1955–1957 V light curve on the 1982–1984 V light curve. The light variations in the 1982–1984 eclipse near the second contact are well defined but near the third contact an anomalous brightening was found (Oki *et al.*, 1984; Boyd *et al.*, 1984). The time of

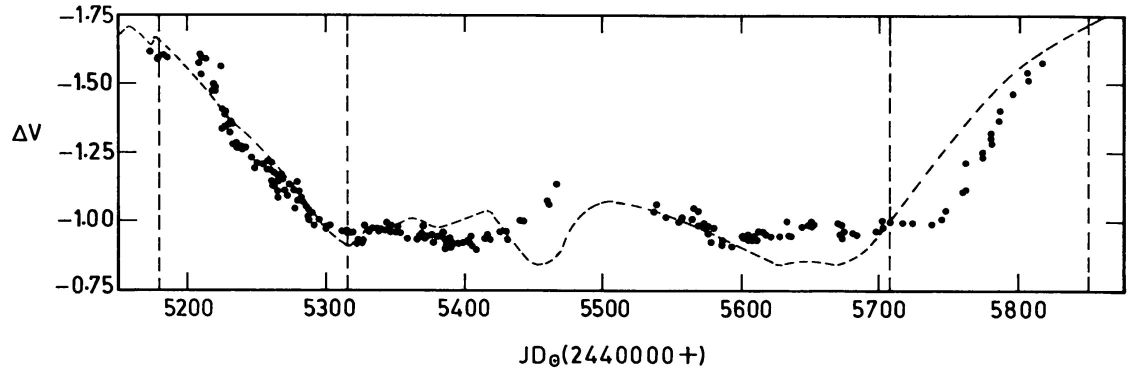

Fig. 4. The 1955–1957 V light curve (dashes) superimposed upon the 1982–1984 (dots) V light curve. The dashed vertical lines indicate the predicted times of contacts.

third contact may be much later than predicted. In Figure 4 we matched the light curves using the pre-eclipse brightness level and the position of the second contact. In the interval JD 2445467 (12 May, 1983) to JD 2445535 (19 July, 1983) ε Aur was very close to the Sun in the sky and, therefore, no photometric data are available. Probably the light variations during this interval are similar to the eclipse-like feature seen near mid-totality in the 1955–1957 eclipse (Gyldenkerne, 1970). But in the 1928 eclipse light curve there is no definite evidence or pattern of eclipse-like feature near mid-totality. However, if we assume that the brightness dip seen around JD 2425660 in Huffer's (1932) 1929 observations is one of the possible eclipse-like feature, then we may conclude that there is a migration of this feature in the 1955–1957 and 1982–1984 eclipse light curves towards later phases with respect to the date of second contact (Figure 4). The brightness dip (around JD 2435560) near mid-totality in the 1955–1957 eclipse is about 80 days duration, whereas the pulsation period is of the order of 60 or 140 days. It may be possible that there is more than one pulsation period in the Cepheid-like variability of the F supergiant. However, the light variations during the totality phase cannot be explained as being due to the pulsation of the primary. The mid-eclipse brightening and downward slope of the totality persists even after correction for the pulsation of the primary. The KI 7700 Å line strength variation also clearly indicate the mid-eclipse brightening (Parthasarathy and Lambert, 1983a, b). The mid-eclipse brightening and the downward slope of the totality are also seen in the 1955–1957 eclipse. The short duration $0^m.1$ to $0^m.2$ variations seen during the totality are also present in the 1955–1957 eclipse totality phase; for example the variations just before the fourth contact (around JD 2435900). These variations appear to repeat from eclipse to eclipse. The light variations during the totality suggest that the eclipsing disk may be clumpy, small-scale localized density irregularities along the length of the disk which may account for the secondary light variations (after correcting for the Cepheid-like variations in the brightness of the primary) observed during the totality.

4. The Colour Variations

In addition to the secondary light variations there are secondary colour variations too. These secondary variations in totality phase persist even after correcting for the Cepheid-like pulsation of the primary. If the eclipsing dusty disk is uniform and composed of material with neutral extinction (independent of wavelength) properties the the colour variations within totality and outside the eclipse should be the same. However, if there is an extended gaseous envelope around the disk, and material with some kind of selective extinction properties in the disk, then the F0 Ia star will undergo colour variations when the disk causes an eclipse.

The average $B - V$ colour before first contact is found to be $+0\overset{m}{.}552$ which is in agreement with the pre-eclipse $B - V$ values given by Blanco *et al.* (1968) and Gyldenkerne (1970).

The *uvby*, *VRI*, and *BV* colour variations during the ingress and early totality phase are shown in Figures 5, 6, and 7, respectively. The $B - V$ colour variation shown in Figure 7 is determined from the observations of HPO and TAO (Hopkins and Stencel, 1983) data. Each data point in Figure 7 is an average of observations of 10–15 day

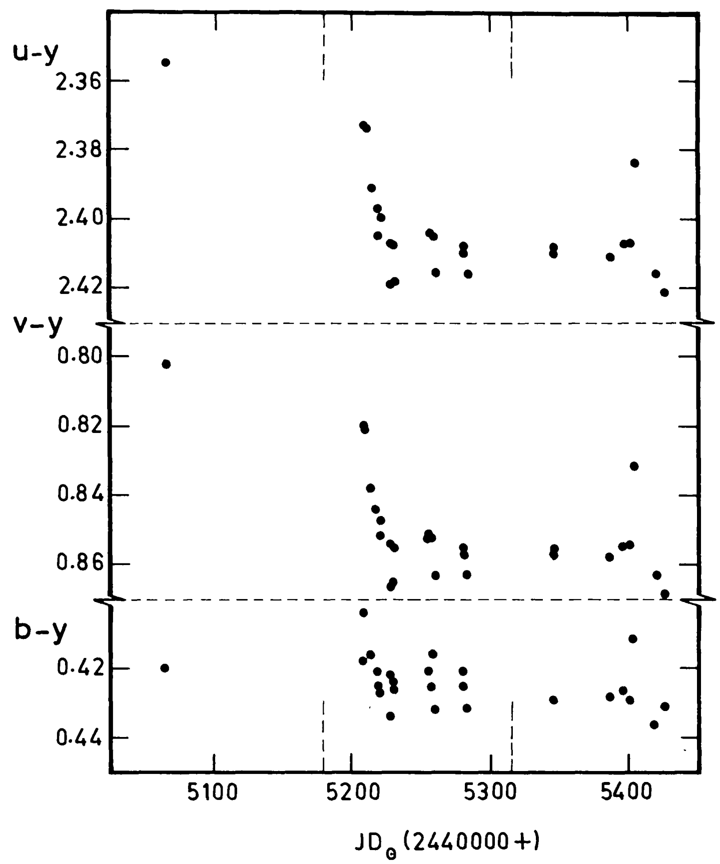

Fig. 5. The *uvby* colour variations of ε Aur during ingress and early totality phases according to observations at the McDonald Observatory.

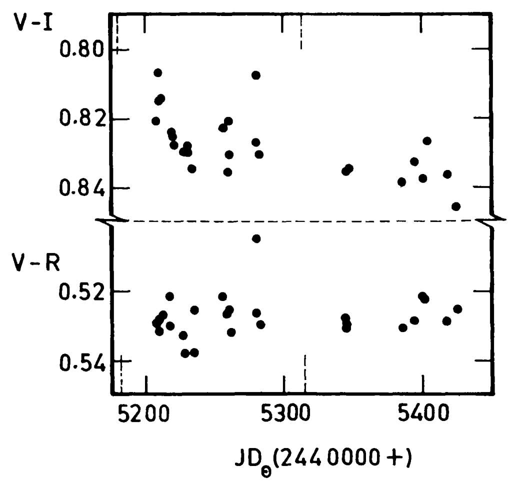

Fig. 6. The *VRI* colour variations of ε Aur during ingress and early totality phases according to observations at the McDonald Observatory.

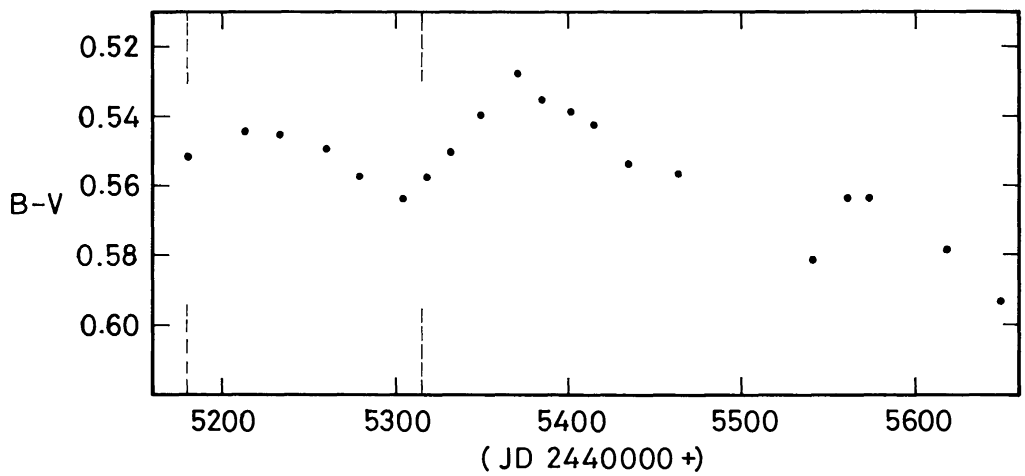

Fig. 7. The $B - V$ colour variations of ε Aur during ingress and totality phases according to HPO and TAO data.

intervals. The colour variations suggest slight increase in the eclipse depth towards shorter wavelengths. The observations of Thiessen (1957), Huruhata and Kitamura (1958), and Stub (1972) suggested that the secondary variations are colour dependent. The colour variations shown in Figures 5–10 suggest that: (i) the eclipse depth is slightly larger in the UV; (ii) the colour indices become slightly redder during the eclipse; (iii) the secondary variations are wavelength dependent.

Analysis of the 1955 eclipse observations of Huruhata and Kitamura (1958) and Widorn (1959) suggest that the colour indices are relatively slightly blue ($\approx 0^{\mathrm{m}}.02$ to $0^{\mathrm{m}}.04$) during ingress phase than during the egress phase. The $B - V$ colour variation shown in Figure 7 suggests a slight increase ($\approx 0^{\mathrm{m}}.01$) in the colour index during ingress phase to second contact phase (JD 2445300) and then a decrease until the commencement of mid-eclipse brightening. The $B - V$ colours after mid-totality (from

JD 2445540) are $0^m.01$ to $0^m.05$ redder than those during the pre-eclipse and early totality phase. The secondary colour variations observed during the totality of the 1982–1984 eclipse are in agreement with the colour variations observed during the totality phase of the 1955–1957 eclipse. Gyldenkerne (1970) from an analysis of the 1955 eclipse data found that the mean colour $B - V$ increased from $0^m.558$ during the first part of the totality to $0^m.572$ after mid-eclipse, and it has a comparatively high value of $0^m.58$ in most parts of the egress phase.

The correlation between the light variations and variations in $B - V$ ($\Delta(B - V) = (B - V) - 0^m.552$) during ingress and early totality phase is shown in Figure 8. A similar analysis of post mid-eclipse and egress phase colour indices will be interesting. We expect post mid-eclipse and egress phases to have $\Delta(B - V)$ values of the order of $+0^m.02$ to $+0^m.05$. We find similar results from an analysis of the narrow band photometric observations of Fredrick (1960) and Huruhata and Kitamura (1958).

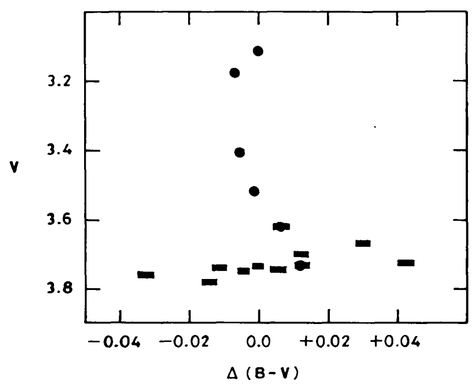

Fig. 8. Correlation between the light variations and colour variations during ingress to mid-totality phases. The abscissa is defined as $\Delta(B - V) = (B - V) - 0.552$.

Fredrick's data is mostly near the third contact and egress phases; the colour variations during this interval are shown in Figure 9. The large variations around JD 2435900 are real and they are noted in the data of Huruhata and Kitamura (see Figure 10) and Thiessen (1957). Huruhata and Kitamura's data are rather scanty, but support the conclusions that the colour indices are redder during egress than during ingress and the large variations around JD 2435900.

The colour variations during the totality in the 1955–1957 eclipse clearly suggest that the post mid-eclipse average colour index is redder than the pre mid-eclipse average colour index and continues to remain so during the rest of the totality phase and also the egress phase. Gyldenkerne (1970) indicated that the selectivity of the secondary variations may not be intimately connected with the primary variations. Canavaggia (1980) ascribed the wavelength-dependent secondary fluctuations of ε Aur to dual origin intrinsic fluctuations of the primary and extinction of a selectively absorbing material. The secondary colour variations during the totality, the downward slope of the totality, and the variations just before the fourth contact appear to repeat from eclipse to eclipse.

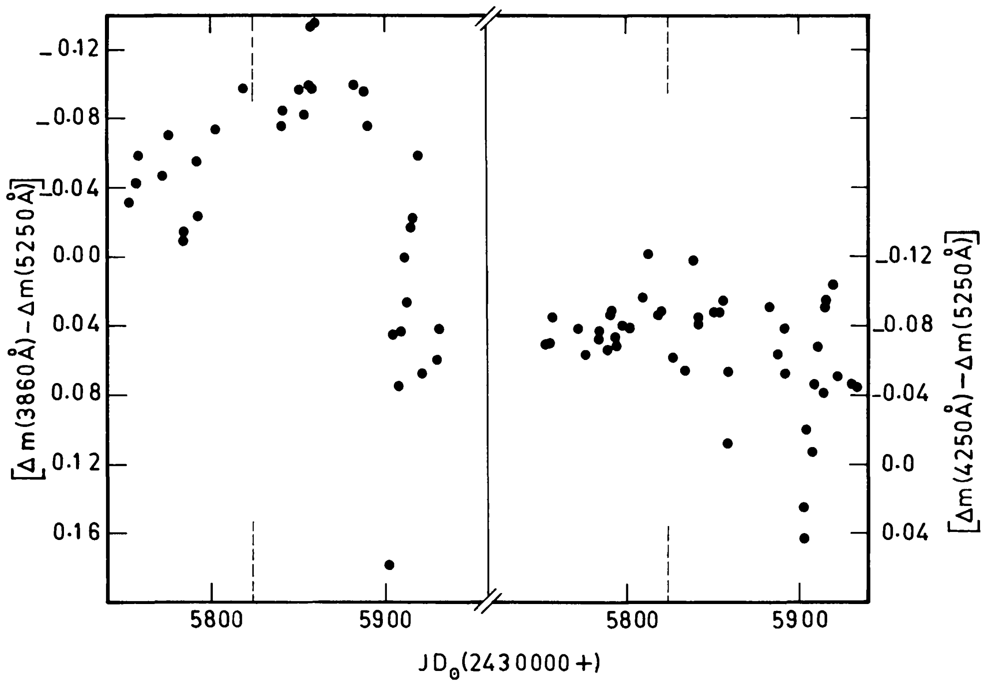

Fig. 9. The narrow band colour variations of ε Aur during the post mid-eclipse and egress phases of the 1955–1957 eclipse. The dashed vertical line indicates the time of third contact. (The observational data are from Fredrick, 1960.)

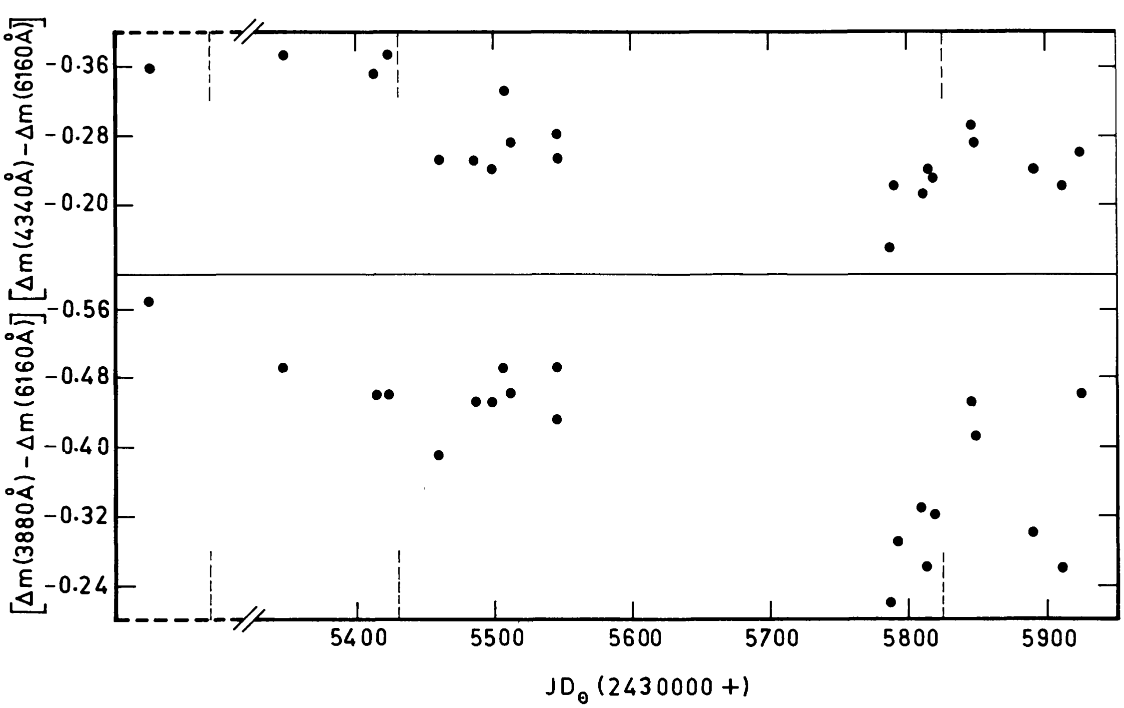

Fig. 10. The narrow band colour variations of ε Aur during ingress, totality, and egress phases of the 1955–1957 eclipse. The dashed vertical lines indicate times of first, second, and third contacts. (The observational data are from Huruhata and Kitamura, 1958).

One can notice these variations in the 1928–1931 and 1955–1957 eclipse light curves.

The slightly deeper eclipse depth in the ultraviolet than at visual wavelengths (Chapman *et al.*, 1983; Parthasarathy and Lambert, 1983c; Ake and Simon, 1983) and an increase in the colour index during the totality, and also the downward slope of the totality suggest some kind of selective extinction of the Fo Ia star light by the disk. However, no significant increase in the strength of the 2200 Å dip is noted during the eclipse. The eclipse depth of $1\overset{m}{.}05$ in the interval 2505–2000 Å is slightly larger than at visual wavelengths (Parthasarathy and Lambert, 1983c). Chapman *et al.* (1983) suggested an envelope of small grains around the secondary to account for the larger eclipse depth in the UV. The effect of an increase in the colour index during the totality appears to be similar to an increase in $E(B - V)$ from $0\overset{m}{.}35$ during the pre-eclipse to $0\overset{m}{.}38$ in totality.

5. Conclusions

The secondary light and colour variations during the totality suggest that: (i) the eclipsing disk is not homogeneous; (ii) the star-like object in the disk is not at the centre of the disk; (iii) the eclipsing disk is tilted with respect to the equatorial plane of the primary, or there is a ring around the primary which is at an angle with respect to the eclipsing disk; (iv) there are relatively less opaque regions or temperature gradients in the disk; (v) the downward slope of the totality repeats from eclipse to eclipse and appears to be connected with the increase in the colour index during the totality; (vii) the gaseous content in the disk in the post mid-eclipse to early egress phase interval may be relatively higher than in the ingress to pre mid-eclipse phase interval. The gaseous content in the disk which gives rise to a shell absorption spectrum during the eclipse may be able to account for the slightly larger eclipse depth in the wavelength interval 1700–4000 Å and a slight increase in the colour index during the eclipse.

From the infrared photometry Backman *et al.* (1984) derived temperature of 500 K for the disk. The IRAS infrared fluxes kindly provided by Pottasch (1985) are: 9.26 Jy (12 μm), 2.8 Jy (25 μm), and 0.53 Jy (60 μm). From the IRAS fluxes and from the 5–20 μm infrared photometry of ε Aur by Backman *et al.* (1984) the temperature of the eclipsing disk is found to be 550 K. The eclipse depth is almost independent of the wavelength from 1700 Å to 4 μm. The eclipse depth decreases with increasing wavelength from 4 to 60 μm and suggests that the eclipsing object is a cold dusty disk with very large grains. In the ultraviolet 1250 Å to 1700 Å the eclipse depth decreases with decreasing wavelength, and the observed UV excess may be due to a star embedded in the disk (Parthasarathy and Lambert, 1983c).

Acknowledgements

We are grateful to Professor Harlan J. Smith, Professor David S. Evans, and Professor Thomas G. Barnes for their kind encouragement and for alloting the observing time. We are thankful to Professor S. R. Pottasch for providing IRAS fluxes of ε Aur. M.P. is thankful to Professor J. C. Bhattacharyya for his kind hospitality.

References

Ake, T. B. and Simon, T.: 1983, *IAU Circ.*, No. 3763.
Backman, D. E., Becklin, E. E., Cruikshank, D. P., Joyce, R. R., Simon, T., and Tokunaga, A.: 1984, *Astrophys. J.* **284**, 799.
Barnes, G. T. and Moffett, T. J.: 1979, *Publ. Astron. Soc. Pacific* **95**, 1012.
Blanco, V. M., Demers, S., Douglass, G. G., and Fitzgerald, M. P.: 1968, *Publ. US Naval Obs.* **XXI**.
Boehm, C., Ferluga, S., and Hack, M.: 1984, *Astron. Astrophys.* **130**, 419.
Boyd, L. J., Genet, R. M., and Hall, D. S.: 1984, *Inf. Bull. Var. Stars*, No. 2562.
Cameron, A. G. W.: 1971, *Nature* **229**, 178.
Canavaggia, R.: 1980, *Astron. Astrophys.* **83**, 105.
Chapman, R. D., Kondo, Y., and Stencel, R. E.: 1983, *Astrophys. J.* **269**, L17.
de Vaucouleurs, G. and Angione, J.: 1974, *Publ. Astron. Soc. Pacific* **86**, 104.
Flin, P., Winiarski, M., and Zola, S.: 1985, *Inf. Bull. Var. Stars*, No. 2678.
Fredrick, L. W.: 1960, *Astron. J.* **65**, 97.
Gyldenkerne, K.: 1970, *Vistas Astron.* **12**, 199.
Hack, M.: 1961, *Mem. Soc. Astron. Ital.*, **32**, 4.
Hack, M. and Selvelli, P. L.: 1979, *Astron. Astrophys.* **75**, 316.
Hopkins, J. L. and Stencel, R. E.: 1983, *Epsilon Aurigae Newsletter*, No. 9.
Huang, S.-S.: 1965, *Astrophys. J.* **141**, 976.
Huffer, C. M.: 1932, *Astrophys. J.* **76**, 1.
Huruhata, M. and Kitamura, M.: 1958, *Tokyo Astron. Bull. II* **102**, 1103.
Kopal, Z.: 1954, *Observatory* **74**, 14.
Kopal, Z.: 1971, *Astrophys. Space Sci.* **10**, 332.
Kuiper, G. P., Struve, O., and Strömgren, B.: 1937, *Astrophys. J.* **86**, 570.
Larsson-Leander, G.: 1958, *Arkiv. Astron.* **2**, 283.
Ludendorff, H.: 1924, *Sitzber. Berlin Preuss. Akad. Wiss.* **9**, 49.
Moffett, T. J. and Barnes, T. G.: 1979, *Astron. J.* **84**, 627.
Oki, T., Sekiya, I., and Hirayama, K.: 1984, *Inf. Bull. Var. Stars*, No. 2496.
Parthasarathy, M. and Lambert, D. L.: 1983a, *IAU Circ.*, No. 3766.
Parthasarathy, M. and Lambert, D. L.: 1983b, *IAU Circ.*, No. 3857.
Parthasarathy, M. and Lambert, D. L.: 1983c, *Publ. Astron. Soc. Pacific* **95**, 1012.
Plavec, M. J.: 1981, in R. D. Chapman (ed.), *The Universe at Ultraviolet Wavelengths, The First Two Years of IUE*, NASA SP-2171, p. 397.
Pottasch, S. R.: 1985, private communication.
Sahade, J. and Wood, F. B.: 1978, *Interacting Binary Stars*, Pergamon Press, New York, p. 152.
Struve, O.: *Publ. Astron. Soc. Pacific* **68**, 27.
Struve, O. and Zebergs, V.: 1962, *Astronomy of the 20th Century*, Macmillian, New York, p. 305.
Stub, H.: 1972, *Astron. Astrophys.* **20**, 161.
Thiessen, G.: 1957, *Z. Astrophys.* **43**, 233.
Widorn, Th.: 1959, *Mitt. Univ. Sternwarte Wien* **10**, 3.
Wilson, R. E.: 1971, *Astrophys. J.* **170**, 529.
Wright, K. O.: 1970, *Vistas Astron.* **12**, 147.